Pacific Graphics 2013
B. Levy, X. Tong, and K. Yin
(Guest Editors)

Volume 32 (2013), Number 7

Improving Memory Space Efficiency of Kd-tree for Real-time Ray Tracing

B. Choi, B. Chang, and I. Ihm

Department of Computer Science and Engineering, Sogang University, Korea

Abstract

Compared with its competitors such as the bounding volume hierarchy, a drawback of the kd-tree structure is that a large number of triangles are repeatedly duplicated during its construction, which often leads to inefficient, large and tall binary trees with high triangle redundancy. In this paper, we propose a space-efficient kd-tree representation where, unlike commonly used methods, an inner node is allowed to optionally store a reference to a triangle, so highly redundant triangles in a kd-tree can be culled from the leaf nodes and moved to the inner nodes. To avoid the construction of ineffective kd-trees entailing computational inefficiencies due to early, possibly unnecessary, ray-triangle intersection calculations that now have to be performed in the inner nodes during the kd-tree traversal, we present heuristic measures for determining when and how to choose triangles for inner nodes during kd-tree construction. Based on these metrics, we describe how the new form of kd-tree is constructed and stored compactly using a carefully designed data layout. Our experiments with several example scenes showed that our kd-tree representation technique significantly reduced the memory requirements for storing the kd-tree structure, while effectively suppressing the unavoidable frame-rate degradation observed during ray tracing.

Categories and Subject Descriptors (according to ACM CCS): I.3.6 [Computer Graphics]: Methodology and Techniques—Graphics data structures and data types I.3.7 [Computer Graphics]: Three-Dimensional Graphics and Realism—Raytracing

1. Introduction

1.1. Background

Thanks to their reliable high performance in the calculation of ray-object intersections, kd-trees are considered one of the most effective acceleration structures for ray tracing. Given a three-dimensional scene, the kd-tree is constructed in a top-down manner by recursively subdividing the scene's voxel space using axis-aligned splitting planes. The timing performance of the resulting kd-tree is affected greatly by the fundamental decisions of where to position the splitting planes and when to stop the recursive subdivision. The surface-area heuristic (SAH), introduced by MacDonald and Booth [MB90], is generally acknowledged as the best strategy for building high-quality kd-trees [Hav01, Wal04], because its simple cost-prediction model based on the theory of geometric probability [San02] usually facilitates reasonably good decision making.

In the standard kd-tree representation, each inner node stores information about the splitting plane and addresses pointing to its two child nodes, while each leaf node stores a list containing indices referring to the triangles that overlap with the voxel referenced by the leaf. This method is used widely but this representation cannot avoid the following inherent problem that arises during the construction of kd-trees. If a triangle in the voxel penetrates a selected splitting plane when a voxel is being subdivided, this triangle is sorted into both subvoxels redundantly, which increases the actual number of triangles handled by the construction algorithm. If this happens frequently, the leaf nodes in the resulting kd-tree have a high frequency of duplicate references to the same triangles. This is known to be a drawback of the kd-tree structure, especially when compared with the bounding volume hierarchy (BVH), in which triangles are generally not shared by leaf nodes, so the resulting binary trees are usually smaller and shallower than the kd-trees.

Table 1 shows that many duplicate triangles are present in the leaf nodes of kd-trees constructed for five representative scenes using the de facto standard SAH-based construction algorithm [WH06]. The *count* column shows the number of

interval	Kitchen (101,015)		Conference (190,947)		Soda Hall (2,167,474)		San Miguel (10,500,551)		Power Plant (12,748,510)	
	count	longest	count	longest	count	longest	count	longest	count	longest
10,001 ∼ 15,000	0	-	0	-	0	-	2	6.395	0	-
5,001 ∼ 10,000	0	-	0	-	0	-	3	4.267	18	139.3
2,001 ∼ 5,000	0	-	1	84.77	0	-	43	5.069	150	73.43
1,001 ∼ 2,000	1	6.265	10	11.77	36	184.6	147	1.276	451	72.85
501 ∼ 1,000	0	-	73	5.029	215	139.0	776	1.020	1,955	63.27
201 ∼ 500	3	3.763	591	2.882	3,131	42.66	4,926	0.398	15,619	36.00
101 ∼ 200	8	0.995	4,100	2.054	4,468	51.36	15,360	0.196	36,530	32.04
51 ∼ 100	50	0.860	6,901	1.808	20,527	34.96	64,113	0.121	85,873	25.38
21 ∼ 50	322	0.315	16,143	1.061	112,036	24.24	364,056	0.076	363,373	15.51
11 ∼ 20	1,782	0.157	22,758	0.521	249,662	16.86	1,151,922	0.047	690,882	10.94
1 ∼ 10	98,849	0.034	140,370	0.353	1,777,399	7.304	8,899,203	0.025	11,553,659	2.625
no. of indices	323,606 (x3.20)		2,752,009 (x14.41)		16,539,116 (x7.63)		77,619,842 (x7.39)		78,550,737 (x6.16)	

Table 1: *Redundant triangles in kd-trees. The figures in parentheses below the scene name indicate the number of triangles in each scene. The figure in the last row shows the total number of triangles actually represented in the leaf nodes of the respective kd-tree, which has a high degree of redundancy.*

triangles in a scene for each *interval*. Compared with the original number of triangles in each scene, the total numbers of indices stored in the leaf nodes of the respective kd-trees, i.e., the *no. of indices*, demonstrate the redundancy problem, which is inevitable in the current kd-tree representation and it may lead to inefficient tree structures.

We tested several scenes and found that most of the triangles in the Kitchen scene, i.e., 98,849 out of 101,015 (97.9%), were small and well tessellated. This was a rather good example because there was *only* a 3.20 times increase in the number of stored references. By contrast, a substantial amount of *ill* triangles in the Conference scene intersected repeatedly with the splitting planes selected by the SAH metric, which produced a high ratio of 14.41. In this table, the figures in the *longest* column denote the average length of the longest edges of triangles in the corresponding frequency range. In many cases, these results show that relatively large and/or skinny triangles generally led to excessive redundancy in the tree structure (refer to Figure 1).

The replication of triangles during kd-tree construction means that the acceleration structure often imposes a non-trivial spatial overhead. This is shown in Table 2, where the size of the kd-trees built using a construction algorithm [WH06] and represented with a compact data structure proposed by Wald [Wal04] are compared with the *normalized* sizes of the geometry data. This analysis and that in the previous table suggest that it would undoubtedly be worthwhile to develop a new kd-tree scheme that facilitates a more compact representation by reducing triangle redundancy.

1.2. Our contribution

In this paper, we propose a space-efficient kd-tree representation method that unlike the standard method, permits the optional storage of a reference to a triangle in the inner nodes. The inherent problem of kd-trees that the tree structure easily grows in size due to duplicate references to the geometry is eased markedly by selecting triangles that cause excessive duplication, and storing them in proper inner nodes, which significantly reduces the memory space to store the redundant references in the leaf nodes.

	no.'s of triangles (K)	no.'s of vertices (K)	size of geom. (MB)	size of kd-tree (MB)
Kitchen	101.0	53.4	2.79	2.94
Conference	190.9	114.3	5.67	21.06
Soda Hall	2,167.5	5,489.8	192.34	131.98
San Miguel	10,500.6	6,093.5	306.13	662.74
Power Plant	12,748.5	5,731.5	320.81	635.22

Table 2: *Relative sizes of the geometry data and kd-trees. Several different representations are possible for a polygonal model with normals and texture coordinates at the vertices. Therefore, we simply assume that they are represented using the 'indexed face set' method to view the spatial overheads of the kd-tree structure, where the* size of geometry *in the table was calculated as (no. of triangles)*12 bytes + (no. of vertices)*32 bytes.*

Our new kd-tree representation method requires a slight modification of the standard kd-tree traversal algorithm (e.g., that summarized in [Hav01,Wal04]), where a ray-triangle intersection computation is required each time an inner node containing a triangle reference is visited, and the first hit in a leaf node is compared to that, if any, between the ray and the triangles of the visited inner nodes. This method is sim-

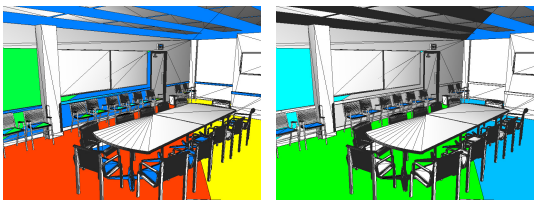

(a) Conference (standard) (b) Conference (ours)

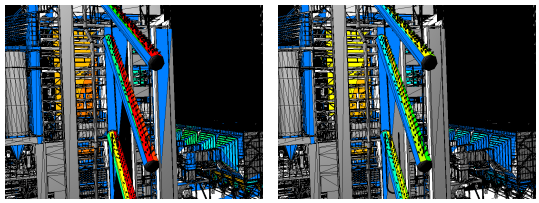

(c) Power Plant (standard) (d) Power Plant (ours)

(e) Color map

Figure 1: *Problematic triangles in kd-trees. For each triangle, the number of duplicates in the kd-tree are color coded in descending order from red (indicating the frequency range [4001 to ∞]) to orange ([2001 to 3000]), yellow ([1401 to 1500]), green ([1001 to 1100]), sky blue ([601 to 700]), and blue ([101 to 500]). As easily understood, relatively large and/or skinny triangles tended to be duplicated repeatedly during kd-tree construction. Unfortunately, it is often difficult to remove these types of triangles during the modeling stage. However, if the inner nodes are allowed to store indices to triangles, as proposed in this paper, this new kd-tree representation (ours) may reduce the redundancy problem substantially compared with the widely accepted representation (standard).*

ple to implement but this extended traversal algorithm may degrade the ray-tracing performance markedly because application of the *early* intersection test to a triangle that has been moved to an inner node often turns out to be unnecessary (compare with the *lazy* intersection test carried out in the standard kd-tree traversal algorithm). Thus, it is important to build an efficient kd-tree that avoids unnecessary early intersection tests as much as possible while maximizing the benefit of the elimination of duplicate references from leaf nodes. To address this problem, we present a kd-tree construction algorithm based on two simple cost metrics, which allows us to effectively determine when and how to choose triangles for inner nodes during kd-tree construction. Then, we explain how the new form of kd-tree is stored efficiently using a compact data layout, which facilitates its efficient runtime execution.

2. Related work

The ray-tracing performance of kd-trees is affected greatly by the way they are constructed, particularly the positioning of the axis-aligned splitting planes during recursive kd-tree construction. Among several possible strategies, the surface area heuristic (SAH) method introduced by MacDonald and Booth [MB90], is generally acknowledged to produce the best kd-trees in terms of ray-tracing speed [Hav01, Wal04]. Several modifications have been made to the SAH-based cost metric [Hav01, HKRS02, Hun08, RKJ96, FFD09, CCI12, WGS04, IH11] to further enhance the temporal performance of SAH kd-trees.

From an algorithmic point of view, Wald and Havran introduced an algorithm constructing a kd-tree in $O(n \log n)$ time, which is the theoretical lower bound [WH06]. Hunt et al. [HMS06], Popov et al. [PGSS06], and Shevtsov et al. [SSK07] presented faster, scanning-based algorithms that approximated the SAH cost function with only slight frame-rate degradation. High construction costs were considered to be a key drawback that prevented kd-trees from being used in the rendering of dynamic scenes. However, fast kd-tree construction is now possible via the effective parallelization of the construction process on modern CPUs and GPUs, as reported previously [ZHWG08, CKL*10, WZL11]. Furthermore, considerable attention has been paid to the development of memory-efficient kd-tree layouts and the optimization of the traversal algorithm for specific hardware (for example, refer to a recent review article [HH11]).

As well as improving the temporal performance, the generation of space-efficient kd-tree structures is equally important because it facilitates effective memory management during ray tracing. However, most attempts to reduce the size of acceleration hierarchies and geometries have focused on other structures such as the BVH and its variants. Mahovsky and Wyvill proposed a hierarchical BVH encoding scheme that reduces the memory requirements by storing the six coordinates of the axis-aligned bounding box of a node relative to its parent node using 4-bit or 8-bit unsigned integers [MW06]. Cline et al. also used lower precision numbers and reduced the size of the resulting BVH further by employing a pointer-free heap-like data structure with a high branching factor [CSE06]. Wächter and Keller also generated compact hierarchies using a lazy building technique [WK06].

To render large models, Lauterbach et al. presented a two-level hierarchy model where lower level hierarchies implicitly encoded those generated from carefully constructed triangle strips [LYTM08]. This idea of a two-level structure was also applied by Segovia and Ernst to the lossy encoding of BVH nodes and their geometries on two levels [SE10]. Bauszat et al. further compressed the BVH using a modified hierarchy known as the minimal bounding volume hierarchy [BEM10]. Kim et al. proposed a cluster-based layout-preserving BVH compression technique, which gave effi-

cient random access to the compressed BVHs [KMKY10]. On the other hand, Hou et al. proposed a construction scheme that builds kd-trees/BVHs for large models effectively on the GPU with limited memory [HSZ*11].

Finally, Havran et al. allowed to link an extra tree structure, built for oversized geometries, as a ternary child of an inner node of a hybrid tree blending a spatial kd-tree (SKD-tree) with bounding volume primitives [HHS06]. While their method mainly focused on fast construction of spatial hierarchies, allowing to store ternary tree structures in the inner nodes often degraded the ray-tracing performance significantly. Our method differs in that only a carefully chosen triangle is stored in an inner node of the standard kd-tree, effectively suppressing the unavoidable frame-rate degradation observed during ray tracing. In order to reduce the search space quickly during ray tracing, Zuniga et al. isolated a *wide* primitive in a voxel as a right child of the corresponding inner node of another hybrid, dual extent tree [ZU06]. However, such strategy usually increased the tree size markedly due to the resulting local unbalance in the tree structure.

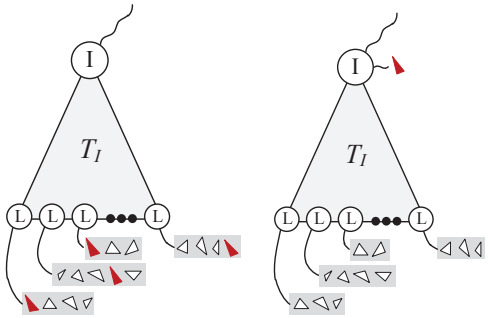

(a) The standard representation (b) Our representation

Figure 2: *Augmented inner nodes. Given a subtree, we have the option of storing a reference to a triangle with high redundancy in the root of the subtree instead of leaving multiple copies in the leaf nodes, which greatly reduces the space needed to represent the subtree.*

3. Construction of space-efficient kd-trees

3.1. Two heuristic metrics for triangle selection

Figure 2 shows the key concept of our method for increasing space efficiency by eliminating highly duplicated references to the same triangles as much as possible. As mentioned in the Introduction, however, storing triangles (i.e., storing references to triangles) in inner nodes may degrade the ray-tracing performance, mainly because it increases the number of unnecessary early calculations of ray-triangle intersections. Thus, the triangles must be selected carefully to greatly reduce the memory requirements while avoiding wasteful computations as much as possible.

Consider a kd-tree T, which is built using a standard SAH-based method, and its subtree T_N, which is rooted in the node N, where the corresponding voxel region is denoted as V_N. The first necessary condition that selects a triangle as a candidate for an inner node I is the likelihood that for a given random ray the triangle will eventually be tested for a ray-triangle intersection, irrespective of whether it is actually hit by the ray or not, during the traversal of T_I. This condition is obvious because a higher likelihood means there is a lower probability that the *early evaluation* of the ray-triangle intersection will turn out to be unnecessary.

Let $\mathcal{T}(T_I)$ denote the set of all triangles stored in the leaf nodes of T_I. We also assume that, given a triangle $t \in \mathcal{T}(T_I)$, $\mathcal{L}(t,T_I)$ represents the set of all leaf nodes of T_I passed by t, where $\mathcal{L}(\cdot,T_I)$ specifically denotes the set of all leaf nodes of T_I. We also define $SA(V)$ as the surface area of the voxel V, so the first surface area-based *occupancy* measure of the inner node I is defined as follows:

$$f_{occu}(t,T_I) = \frac{\sum_{L\in\mathcal{L}(t,T_I)} SA(V_L)}{\sum_{L\in\mathcal{L}(\cdot,T_I)} SA(V_L)},$$

where the numerator, i.e., the sum of the geometric probability that each leaf node intersecting with the triangle t will be hit by a random ray, is normalized between 0 and 1. Note that, if a leaf intersecting with the triangle t is reached during ray tracing, a ray-triangle intersection calculation is incurred with respect to t. Therefore, this occupancy measure provides a good estimate of the chance that a ray-triangle intersection computation for t occurs during the traversal of T_I. Only storing a triangle with a sufficiently high occupancy measure in the inner node may reduce the timing penalty incurred by unnecessary ray-triangle intersection calculations at inner nodes.

We apply a second requisite condition that a triangle is culled from the leaf nodes of a subtree if its effect in terms of data compression is sufficiently high. Placing a triangle on an inner node inevitably leads to inefficiencies during tree traversal. Thus, we require that a triangle is selected on an inner node only if eliminating the triangle from the leaves results in an adequate reduction in the data size. To implement this condition, we define the following simple *frequency* measure, which determines how frequently the triangle t appears in the leaf nodes of T_I:

$$f_{freq}(t,T_I) = \frac{|\mathcal{L}(t,T_I)|}{|\mathcal{L}(\cdot,T_I)|}.$$

Based on these two metrics, we define an oracle function $pick\_triangle(T_I)$ as follows, which selects a triangle from T_I if an eligible one is available, whereas it returns a null value if not. First, we enumerate the triangles in T_I with an occupancy measure $f_{occu}(t,T_I)$ greater than a given occupancy threshold τ_{occu} in a nonincreasing order. We check each triangle until we find one with a frequency measure $f_{freq}(t,T_I)$ greater than a preset frequency threshold τ_{freq}. A suitable triangle is returned only if one is available.

3.2. The new kd-tree construction algorithm

Now, a new kd-tree can be constructed by a simple recursive process using our rule for choosing a problematic triangle from a subtree. Starting with a kd-tree T constructed for the triangle set $\mathcal{T}_S$ of an input scene S using a standard SAH-based construction algorithm, we examine a given tree T_I, whose root node I is not a leaf, to evaluate the oracle function $pick\_triangle(T_I)$. If an eligible triangle is not found, the tree building process stops. However, if a triangle t is selected from $\mathcal{T}(T_I)$ for culling, where $\mathcal{T}(T_I)$ is the set of triangles in the leaves of T_I, a new SAH-based kd-tree T_I^* is built from $\mathcal{T}(T_I) - \{t\}$, replacing T_I. After t is stored in the root node of T_I^*, the same process is applied recursively to the subtree rooted in each child of the root node of T_I^*.

Algorithm 1 describes an iterative version of this recursive algorithm where direct stack manipulation provides higher runtime performance. When implementing this algorithm, we need to ensure that we do not generate kd-trees containing excessive amounts of triangles placed on the inner nodes. These trees are favorable for memory reduction, but they may tend to slow down ray tracing markedly because they incur a high frequency of, possibly unnecessary, early ray-triangle intersection calculations on the inner nodes. In our method, we allow a triangle t to be stored in an inner node I only if the number of triangles including t, evaluated by the function $count\_triangles(I)$ in Line 8, which are placed on inner nodes on the path from the node I to the root node, does not exceed a preset threshold max_{t2rn} (the subscript *t2rn* denotes the triangles to the root node). In general, our preliminary experiments showed that setting max_{t2rn} to 4 generated effective kd-trees with a good balance between size and speed.

Algorithm 1 Iterative kd-tree construction

```
 1: Build an SAH-based kd-tree T for T_S;
 2: push(root_node(T));
 3: while (stack is not empty) do
 4:    I = pop();
 5:    if ((t = pick_triangle(T_I)) != NULL) then
 6:       Build an SAH-based kd-tree T_I* for T(T_I) − {t};
 7:       Replace T_I with T_I*, and place t on I;
 8:       if (count_triangles(I) == max_t2rn) then
 9:          continue; {Skip the subtrees of T_I*.}
10:       end if
11:    end if
12:    if (rchild_node(T_I*) is not a leaf node) then
13:       push(rchild_node(T_I*));
14:    end if
15:    if (lchild_node(T_I*) is not a leaf node) then
16:       push(lchild_node(T_I*));
17:    end if
18: end while
19: return T;
```

3.3. Kd-tree node layouts for effective storage

To maximize the benefits of our proposed kd-tree scheme, it is important to design effective data layouts for specific types of kd-tree nodes. Our data structure extends the idea of a compact kd-tree representation with efficient caching and prefetching, which was presented in Wald [Wal04], where each inner or leaf node is stored in a unified data layout with 8 bytes. However, our compact kd-tree representation scheme requires that different types of information are additionally stored in the inner and leaf nodes, so the actual data structure is slightly more complicated than that used in [Wal04].

In our framework, the three least significant bits, known as *the layout type indicator*, are reserved for all data layouts and this determines the type of a given 8-byte node (see Figure 3). If the indicator `A` has a value of `000`, `001`, or `010`, the layout represents the *standard* inner node with no reference to a triangle (this is known as a *type I inner node*). In this case, similar to [Wal04], the two lower bits of `A` and the most significant 32 bits of the layout, `B`, denote the dimension and the position of the splitting plane, respectively, while the remaining 29-bit field, `C`, stores the offset of the left child (note that the offset is always a multiple of eight, while the right child always follows the left child).

If the layout type indicator has a flag of `100`, `101`, or `110`, the layout represents the inner node where a triangle reference is stored (*type II inner node*). The meaning of the other bit fields is the same as the standard inner node, except the 8 bytes indicated by the offset field `C` store information for the reference, which are followed by the left and right children. The reference to a triangle is specified in *the T-reference node* with a layout type indicator value of `111`, where an unsigned integer type index in the upper 32 bits of the layout, `D`, points to a triangle in the array of triangles (see Figure 3(b)). The lower 32 bits including the indicator are not used currently, but they are allocated for an 8-byte alignment (note that the 3-bit field of the indicator is reserved for a consistent data structure, but it is not essential). They are not used at present, but these bits could be explored in a future extension. For example, if the storage of two triangles was permitted per inner node, the index to the extra triangle could be stored there.

Similar to inner nodes, our scheme supports two different types of leaf nodes, which leads to a significant additional reduction in the memory space required to store the indices of the triangles found in the leaves. The leaf nodes share the same layout type indicator, i.e., `011`, but they are categorized based on *the 2-bit leaf-mode indicator*, `E`. If a leaf node has the indicator value `00` (refer to Figure 3(c)), it is found in *the 4-byte mode*, while information on the list of triangles for a leaf node is found in a 4-byte triangle index list: i.e., an array of 4-byte unsigned integers specifying the indices in the array of triangles. This format is basically the same as the data layout in [Wal04] where the 32 bits, `F`, and

(a) An inner node: `A = 000/001/010` (type I), or `A = 100/101/110` (type II)

(b) A T-reference node: `A = 111`

(c) A leaf node (4-byte mode): `A = 011` and `E = 00`

(d) A leaf node (2-byte mode): `A = 011` and `E = 01`

Figure 3: *Data layouts for kd-tree nodes. As in [Wal04], a unified layout based on 8 bytes is used for efficient memory access, which represents various types of kd-tree nodes. In our scheme, the type of node is categorized based on the 3-bit layout indicator* `A` *and the 2-bit leaf-mode indicator* `E`*.*

the following 27 bits, `G`, indicate the first item in the array and the number of triangles sorted in the leaf, respectively.

The final layout is the leaf node in *the 2-byte mode*, which is indicated by the leaf-mode indicator value `01` (refer to Figure 3(d)). A leaf node generally contains a few triangles that are frequently stored in the array of triangles with high spatial coherence. This implies that their 4-byte unsigned integer type indices frequently share the same upper 16 bits with only the lower 16 variable bits. To compress the memory space required by the indices, we allocate an extra triangle index list where 2-byte elements store the lower 16 bits of the indices.

Similar to the 4-byte mode, the 32-bit field `F` and the 11-bit field `H` represent the pointer to the first item in the new list and the corresponding number of triangles, respectively. The actual index to the array of triangles is reconstructed easily when combined with the higher 16 bits shared in the bit field `I`. The effect of using the new leaf type on memory space reduction is generally very encouraging. For example, if the Conference scene was represented in our format, only 140,177 out of 1,705,325 triangle indices in the leaves of a kd-tree would be stored in the 4-byte mode whereas the triangle indices of the other 1,565,148 indices would be stored in a compressed form in the 2-byte array (see the *ours (f)* row in Table 3(a)).

4. Experimental results

We fully implemented our kd-tree representation scheme and compared the new kd-trees with those produced using the construction algorithm [WH06] and the compact data layout [Wal04], which we refer to as *standard* kd-trees. In our experiments, we used five scenes with low to high geometric complexity and tested three different camera views per scene to facilitate a robust comparison between different kd-tree techniques (see Figure 4). Unless stated otherwise, all of the evaluations were performed using a PC with dual 3.46 GHz Intel Xeon six-core CPUs and an NVIDIA GeForce GTX 580 GPU. The rendering frame rate was measured while rendering a 1024×1024 image using full ray tracing with 1- or 12-threaded 4×4 SIMD ray packets on the CPU and CUDA blocks with 4×32 threads on the GPU.

As described in Section 3, three major parameters can af-

(a) Kitchen (101,015 triangles)

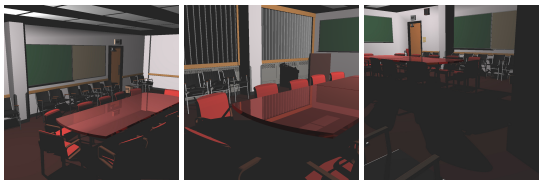

(b) Conference (190,947 triangles)

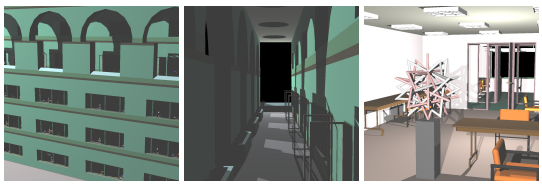

(c) Soda Hall (2,167,474 triangles)

(d) San Miguel (10,500,551 triangles)

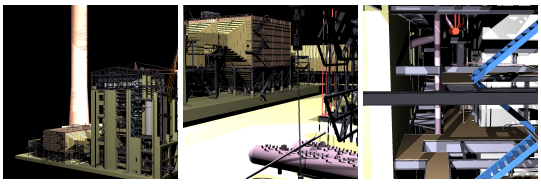

(e) Power Plant (12,748,510 triangles)

Figure 4: *Example scenes and the camera views tested.*

fect the construction of the new kd-trees: i.e., two thresholds, τ_{occu} and τ_{freq}, control the selection of a triangle from a given subtree, while an integer, max_{t2rn}, limits the maximum number of inner nodes along a path to the root node that can hold a triangle. The graphs shown in Figure 5 illustrate typical patterns of the performance variation found with our kd-trees with different combinations of τ_{occu} and τ_{freq}. First, for a given occupancy threshold (*occupancy* in the graph), the effect of kd-tree-size reduction declined as the frequency threshold increased (*frequency* in the graph). This was obvious because a higher frequency threshold would make it difficult to pick triangles for inner nodes. Second, the same trend was observed when increasing the occupancy threshold, although this was less obvious, which suggests that the reduction of the kd-tree size relative to a standard kd-tree was more sensitive to the frequency parameter than the occupancy parameter. Third, the frame-rate degradation when an image was ray-traced using a new kd-tree also decreased as the two threshold values increased. This phenomenon is also easy to understand because the sparse distribution of triangles on the inner nodes due to large threshold values minimizes the waste of computational resources caused by unnecessary early ray-triangle intersection calculations. Therefore, it is particularly important to set the occupancy threshold at a sufficiently high value to maintain the frame-rate degradation at a consistently low level.

Given these results, we tested two different combinations of the two thresholds where max_{t2rn} was set to 4. In the first, a higher priority was given to a reduction of the frame-rate degradation: i.e., $(\tau_{occu}, \tau_{freq}) = (0.9, 0.7)$. In the second, we aimed to achieve greater kd-tree-size reduction while maintaining the frame-rate degradation at an acceptably low level: i.e., $(0.5, 0.4)$. The two subtables in Table 3 show the experimental results, where *ours (f)* and *ours (s)* correspond to the kd-trees for the first and second combinations, respectively. Table 3(a) shows that the number of kd-tree nodes decreased markedly because highly redundant triangles were moved from leaf nodes to inner nodes so the kd-trees were shorter in height, which is discussed later, and they also required less memory space for storage (the number of triangles stored in the inner nodes are specified in the *t-inner* column). In addition, the use of less restrictive thresholds allowed us to control the construction process effectively to create a kd-tree with a smaller number of nodes.

As expected, culling redundant triangles from the leaf nodes significantly increased spatial coherence in the triangle list between the triangles intersecting with a common leaf node, which facilitated the storage of a substantial proportion of the triangle indices in the 2-byte mode (compare the figures in the *4-byte mode* and *2-byte mode* columns). The 2-byte mode technique could also be used for storing a standard kd-tree, but its effect was less significant due to worse locality of triangle reference (observe the decrease in the number of triangle indices in the *total* column). Overall, we achieved a kd-tree-size reduction of 26.4% to 46.1% during the fast rendering-preferred kd-trees (*ours (f)*) and 32.2% to 56.4% for the small size-preferred kd-trees (*ours (s)*).

By contrast, the second table (b) of Table 3 shows the temporal performance of the new kd-trees in terms of frame-rate variation when a 1024×1024 image was rendered by full ray tracing. The timing results showed that the application of the fast rendering-preferred parameters (*ours (f)*) resulted in less than 3.8% (the Soda Hall scene) to 6.9% (the Power Plant scene) frame-rate degradation compared with the standard kd-trees, which was quite encouraging given that the storage of triangles in the inner nodes may incur unnecessary ray-triangle intersection computations and it also degrades the parallel performance of kd-tree traversal on the CPU and GPU because of the introduction of additional branch tests in the inner nodes. When size reduction was preferred (*ours (s)*), the frame-rate drop increased due mainly to the increased number of early ray-triangle intersection calculations, although it was usually below 9.8% (the Conference scene) to 12.5% (the San Miguel scene), which may be acceptable in many situations given the reduced memory sizes.

Note that culling triangles from the leaf nodes also contracted the kd-trees. The two example distributions shown in Figure 6 illustrate the common patterns of changes in the frequencies of leaf node depths when a different type of kd-tree was employed. First, the maximum depth, i.e., the height of the kd-tree, decreased from 181 (the standard kd-tree) to 87 (the fast rendering-preferred kd-tree) and 71 (the small size-preferred kd-tree) for the Soda Hall scene, and from 75 to 62 and 57, respectively, for the San Miguel scene. Second, the peak of the distribution tended to move slightly to the left, where significant frequency reductions were made. Naturally, the shorter structures decreased the kd-tree traversal cost during ray tracing. Frequently, we observed that the frame-rate drops with the new kd-trees were markedly smaller on the GPU than the CPU, particularly in the Conference and Soda Hall scenes (see Table 3 again). This may be because the kd-tree contraction had a more positive impact on the GPU ray-tracer, probably because the GPU is generally more vulnerable to frequent, costly divergent branches during kd-tree traversal. However, this phenomenon appeared to be quite complex.

Finally, we achieved very good performance when the value of the max_{t2rn} parameter was set to 4, although it was not always the best, but it provided a balance between the ray-tracing speed and kd-tree-size reduction. If a larger value was used, the additional compression effect was generally insignificant, which was probably because the fixed τ_{occu} and τ_{freq} values tended to restrict the selection of additional triangles from subtrees at lower levels. The kd-trees usually behaved rather unexpectedly if a value less than 4 was used.

5. Concluding remarks

The main aim of this work was to select triangles that were duplicated in an excessive number of the leaf node voxels

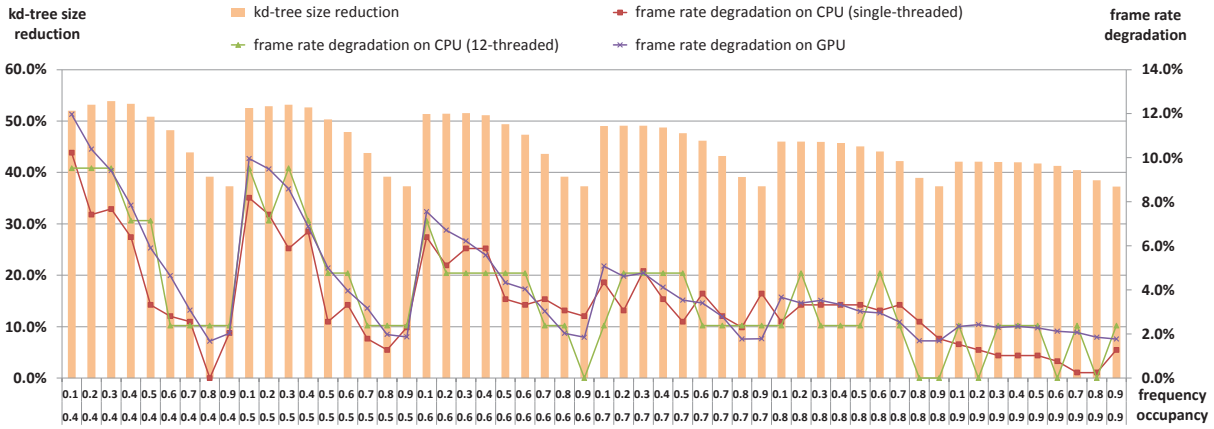

Figure 5: *The effects of varying the occupancy and frequency thresholds on the spatial and temporal performances of the new kd-trees. The experimental results obtained for the Soda Hall scene where max_{t2rn} was set to 4 show the typical variations in the performance patterns. The* kd-tree size reduction *represents the memory size reduction with the new kd-tree relative to the standard form, while the* frame-rate degradation *indicates the corresponding slowdown rate for the ray-tracing frame rate.*

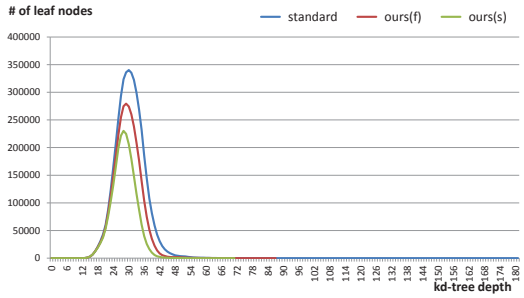

(a) Soda Hall

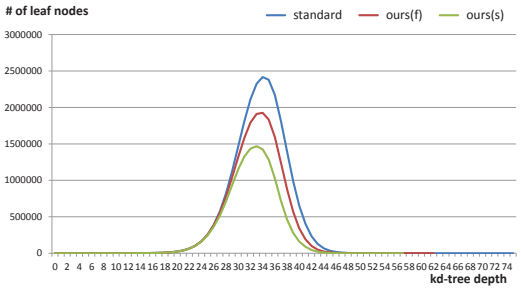

(b) San Miguel

Figure 6: *Contraction of kd-trees ($max_{t2rn} = 4$). We compared the frequency distribution of the leaf node depths of the three types of kd-trees and there was a clear reduction in height when the new kd-tree representation was applied.*

during kd-tree construction, and store them in appropriate inner nodes to avoid redundancy. The experimental results

method	Kitc.	Conf.	Soda H.	San M.	Pow. P.
std.	1.4	2.7	27.4	249.2	286.0
ours (f)	5.2	8.6	54.4	1,671.5	2,283.6
ours (s)	5.0	7.0	60.2	1,323.8	1,825.6

Table 4: *Kd-tree construction times (sec.). The construction algorithms were run on a 3.1 GHz Intel Xeon eight-core CPU, but the runtimes could be reduced greatly by using GPU algorithms such as [ZHWG08, HSZ* 11, WZL11].*

indicated that our method provided a significant kd-tree-size reduction while avoiding any serious degradation of the timing performance by carefully selecting the triangles.

As implied in Table 4, our method is currently limited to static scenes because the kd-tree construction algorithm requires the repeated application of the standard SAH-based construction process [WH06], which is needed for estimating the occupancy of triangles in a voxel. The occupancy measure might also be approximated in terms of the area of the triangle clipped to the current voxel (the theory of geometric probability [San02] states that the probability of a triangle being hit by a random ray is proportional to the area of the triangle). If we could develop an effective occupancy measure that does not require the construction of an SAH-based kd-tree, a simple modification of the standard kd-tree construction algorithm might generate space-efficient kd-trees very quickly.

Dynamic scenes are used widely nowadays, but the construction of space-efficient kd-trees is still important for static scenes, particularly when large ones are ray-traced. We tested a larger scene that was built by duplicating the

Power Plant scene three times (38.2 million triangles), and, similar to the results in the previous section, achieved a kd-tree-size reduction of 35.2% and 36.9% (from 2,181.9 MB to 1,414.1 MB and 1,377.2 MB) for two different threshold pairs, while the respective frame-rate degradation was 2.9% and 5.8% on average (the single-thread mode) for three different views, which indicates the potential of our method for very complex scenes. Note that our method only encodes the acceleration structure but the scene geometry also requires a substantial amount of memory space. Therefore, combining our technique with proper quantization and/or geometry compression techniques would have a great synergistic effect for the ray tracing of very large polygonal models.

Acknowledgments

This work was supported by the National Research Foundation of Korea (NRF) grant funded by the Korea government (MOE) (No. 2012R1A1A2008958). The test scenes are courtesy of Joachim Helenklaken (Kitchen), Anat Grynberg and Greg Ward (Conference), the UC Berkeley Walkthrough Group (Soda Hall), Guillermo M. Leal Llaguno (San Miguel), and the UNC GAMMA group (Power Plant).

References

[BEM10] BAUSZAT P., EISEMANN M., MAGNOR M.: The minimal bounding volume hierarchy. In *Proc. Vision, Modeling, and Visualization '10* (2010), pp. 227–234. 3

[CCI12] CHOI B., CHANG B., IHM I.: Construction of efficient kd-trees for static scenes using voxel-visibility heuristic. *Computers & Graphics 36*, 1 (2012), 38–48. 3

[CKL*10] CHOI B., KOMURAVELLI R., LU V., SUNG H., BOCCHINO R., ADVE S., HART J.: Parallel SAH k-D tree construction. In *Proc. High Performance Graphics '10* (2010), pp. 77–86. 3

[CSE06] CLINE D., STEELE K., EGBERT P.: Lightweight bounding volumes for ray tracing. *Journal of Graphics, GPU, and Game Tools 11*, 4 (2006), 61–71. 3

[FFD09] FABIANOWSKI B., FOWLER C., DINGLIANA J.: A cost metric for scene-interior ray origins. In *Proc. Eurographics '09 Short Papers* (2009), pp. 49–52. 3

[Hav01] HAVRAN V.: *Heuristic Ray Shooting Algorithms*. PhD thesis, Czech Technical University, 2001. 1, 2, 3

[HH11] HAPALA M., HAVRAN V.: Review: Kd-tree traversal algorithms for ray tracing. *Computer Graphics Forum 30*, 1 (2011), 199–213. 3

[HHS06] HAVRAN V., HERZOG R., SEIDEL H.-P.: On the fast construction of spatial hierarchies for ray tracing. In *Proc. IEEE Symposium on Interactive Ray Tracing* (2006), pp. 71–80. 4

[HKRS02] HURLEY J., KAPUSTIN A., RESHETOV A., SOUPIKOV A.: Fast ray tracing for modern general purpose CPU. In *Proc. Graphicon* (2002), p. 2002. 3

[HMS06] HUNT W., MARK W. R., STOLL G.: Fast kd-tree construction with an adaptive error-bounded heuristic. In *Proc. IEEE Symposium on Interactive Ray Tracing* (2006), pp. 81–88. 3

[HSZ*11] HOU Q., SUN X., ZHOU K., LAUTERBACH C., MANOCHA D.: Memory-scalable GPU spatial hierarchy construction. *IEEE Transactions on Visualization and Computer Graphics 17*, 4 (2011), 466–474. 4, 8

[Hun08] HUNT W.: Corrections to the surface area metric with respect to mail-boxing. In *Proc. IEEE Symposium on Interactive Ray Tracing* (2008), pp. 77–80. 3

[IH11] IZE T., HANSEN C.: RTSAH traversal order for occlusion rays. *Computer Graphics Forum 30*, 2 (2011), 297–305. 3

[KMKY10] KIM T., MOON B., KIM D., YOON S.: RACBVHs: Random accessible compressed bounding volume hierarchies. *IEEE Transactions on Visualization and Computer Graphics 16*, 2 (2010), 273–286. 4

[LYTM08] LAUTERBACH C., YOON S., TANG M., MANOCHA D.: ReduceM: Interactive and memory efficient ray tracing of large models. *Computer Graphics Forum 27*, 4 (2008), 1313–1321. 3

[MB90] MACDONALD J., BOOTH K.: Heuristics for ray tracing using space subdivision. *The Visual Computer 6* (1990), 153–166. 1, 3

[MW06] MAHOVSKY J., WYVILL B.: Memory-conserving bounding volume hierarchies with coherent raytracing. *Computer Graphics Forum 25*, 2 (2006), 173–182. 3

[PGSS06] POPOV S., GÜNTHER J., SEIDEL H.-P., SLUSALLEK P.: Experiences with streaming construction of SAH KD-trees. In *Proc. IEEE Symposium on Interactive Ray Tracing* (2006), pp. 89–94. 3

[RKJ96] REINHARD E., KOK A., JANSEN F. W.: Cost prediction in ray tracing. In *Proc. Eurographics Workshop on Rendering Techniques '96* (1996), pp. 41–50. 3

[San02] SANTALO L.: *Integral Geometry and Geometric Probability*. Cambridge University Press, 2002. 1, 8

[SE10] SEGOVIA B., ERNST M.: Memory efficient ray tracing with hierarchical mesh quantization. In *Proc. Graphics Interface '10* (2010), pp. 153–160. 3

[SSK07] SHEVTSOV M., SOUPIKOV A., KAPUSTIN A.: Highly parallel fast KD-tree construction for interactive ray tracing of dynamic scenes. *Computer Graphics Forum 26*, 3 (2007), 395–404. 3

[Wal04] WALD I.: *Realtime Ray Tracing and Interactive Global Illumination*. PhD thesis, Saarland University, 2004. 1, 2, 3, 5, 6, 10

[WGS04] WALD I., GUNTHER J., SLUSALLEK P.: Balancing considered harmful - faster photon mapping using the voxel volume heuristic. *Computer Graphics Forum 23*, 3 (2004), 595–603. 3

[WH06] WALD I., HAVRAN V.: On building fast kd-trees for ray tracing, and on doing that in O(Nlog N). In *Proc. IEEE Symposium on Interactive Ray Tracing* (2006), pp. 61–69. 1, 2, 3, 6, 8, 10

[WK06] WÄCHTER C., KELLER A.: Instant ray tracing: The bounding interval hierarchy. In *Proc. EUROGRAPHICS Symposium on Rendering '06* (2006), pp. 139–149. 3

[WZL11] WU Z., ZHAO F., LIU X.: SAH KD-tree construction on GPU. In *Proc. High Performance Graphics '11* (2011), pp. 71–78. 3, 8

[ZHWG08] ZHOU K., HOU Q., WANG R., GUO B.: Real-time KD-tree construction on graphics hardware. *ACM TOG 27*, 5 (2008), 1–11. 3, 8

[ZU06] ZUNIGA M., UHLMANN J.: Ray queries with wide object isolation and the DE-tree. *Journal of Graphics, GPU, and Game Tools 11*, 3 (2006), 27–45. 4

(a) Statistics related to the kd-tree size. In this table, *t-inner* indicates the new type of inner nodes that hold references to triangles, while the figures in parentheses in the rightmost column represent the size reduction of the new kd-tree relative to the standard SAH-based kd-tree.

scene	tree rep.	no. of kd-tree nodes				no. of indices to triangles			used memory (MB)
		inner	t-inner	leaf	total	4-byte mode	2-byte mode	total	
Kitchen (101,015)	std.	112,100	0	112,101	224,201	323,606	0	323,606	2.9
	ours (f)	87,711	11,923	99,635	199,269	12,570	265,761	278,331	2.2 (26.4%)
	ours (s)	50,616	32,859	83,476	166,951	10,369	227,220	237,589	2.0 (32.2%)
Conference (190,947)	std.	692,332	0	692,333	1,384,665	2,752,009	0	2,752,009	21.1
	ours (f)	356,436	104,548	460,985	921,969	140,177	1,565,148	1,705,325	11.4 (46.1%)
	ours (s)	197,930	142,872	340,803	681,605	117,488	1,280,786	1,398,274	9.2 (56.4%)
Soda Hall (2,167,474)	std.	4,514,974	0	4,514,975	9,029,949	16,539,116	0	16,539,116	132.0
	ours (f)	2,765,685	600,247	3,365,933	6,731,865	427,739	11,026,989	11,454,728	78.6 (40.4%)
	ours (s)	1,288,647	1,132,261	2,420,909	4,841,817	326,192	8,230,869	8,557,061	62.5 (52.6%)
San Miguel (10,500,551)	std.	24,028,541	0	24,028,542	48,057,083	77,619,842	0	77,619,842	662.7
	ours (f)	15,596,361	3,213,304	18,809,666	37,619,331	15,856,444	42,257,800	58,114,244	452.6 (31.7%)
	ours (s)	7,915,317	6,186,060	14,101,378	28,202,755	13,472,086	33,806,033	47,278,119	378.2 (42.9%)
Power Plant (12,748,510)	std.	21,992,127	0	21,992,128	43,984,255	78,550,737	0	78,550,737	635.2
	ours (f)	13,770,505	3,030,957	16,801,463	33,602,925	8,984,545	46,722,160	55,706,705	402.9 (36.6%)
	ours (s)	7,326,642	5,649,934	12,976,577	25,953,153	7,628,722	38,600,428	46,229,150	343.8 (45.9%)

(b) Statistics related to the ray-tracing time (fps). For the CPU, the timings were measured in a single-thread mode (*CPU1*) and a 12-thread mode (*CPU12*) using dual 6-core CPUs. The figures in parentheses represent the increase in the ray-tracing time with the new kd-tree relative to the standard SAH-based kd-tree. The frame rates marked with an asterisk were measured using an NVIDIA Quadro 6000 GPU because the standard SAH trees and the geometry data would not fit into the memory of the NVIDIA GeForce GTX 580 GPU.

scene	tree rep.	Camera view 1			Camera view 2			Camera view 3		
		CPU1	CPU12	GPU	CPU1	CPU12	GPU	CPU1	CPU12	GPU
Kitchen (101,015)	std.	0.867	8.621	16.448	0.959	8.772	20.388	0.709	6.536	11.489
	ours (f)	0.854 (1.6%)	8.403 (2.6%)	15.971 (3.0%)	0.949 (1.1%)	8.696 (0.9%)	19.396 (5.1%)	0.700 (1.3%)	6.410 (2.0%)	11.189 (2.7%)
	ours (s)	0.794 (9.2%)	7.874 (9.5%)	15.009 (9.6%)	0.878 (9.2%)	8.000 (9.6%)	18.242 (11.8%)	0.657 (7.9%)	5.988 (9.2%)	10.545 (9.0%)
Conference (190,947)	std.	1.852	18.868	24.131	1.689	16.393	22.933	2.024	19.608	26.332
	ours (f)	1.828 (1.3%)	18.182 (3.8%)	23.895 (1.0%)	1.634 (3.4%)	15.625 (4.9%)	22.695 (1.0%)	1.961 (3.2%)	18.868 (3.9%)	26.044 (1.1%)
	ours (s)	1.727 (7.2%)	17.241 (9.4%)	23.083 (4.5%)	1.555 (8.6%)	15.152 (8.2%)	22.054 (4.0%)	1.869 (8.3%)	17.857 (9.8%)	25.361 (3.8%)
Soda Hall (2,167,474)	std.	1.248	11.364	14.638	1.395	12.658	19.975	0.454	4.132	5.123
	ours (f)	1.209 (3.2%)	10.989 (3.4%)	14.397 (1.7%)	1.374 (1.5%)	12.195 (3.8%)	19.378 (3.1%)	0.442 (2.8%)	3.984 (3.7%)	5.496 (-6.8%)
	ours (s)	1.135 (10.0%)	10.309 (10.2%)	13.687 (6.9%)	1.276 (9.3%)	11.364 (11.4%)	18.241 (9.5%)	0.430 (5.5%)	3.906 (5.8%)	5.471 (-6.4%)
San Miguel (10,500,551)	std.	0.102	1.016	2.576*	0.153	1.406	3.321*	0.285	2.584	4.744*
	ours (f)	0.097 (5.1%)	0.965 (5.3%)	2.473* (4.2%)	0.149 (2.8%)	1.364 (3.1%)	3.166* (4.9%)	0.277 (3.1%)	2.519 (2.6%)	4.511* (5.2%)
	ours (s)	0.091 (12.5%)	0.907 (12.1%)	2.307* (11.7%)	0.138 (11.0%)	1.297 (8.4%)	3.016* (10.1%)	0.255 (11.8%)	2.387 (8.3%)	4.330* (9.6%)
Power Plant (12,748,510)	std.	0.421	3.497	11.458*	0.522	4.444	6.842*	1.229	11.111	16.092*
	ours (f)	0.424 (-0.7%)	3.401 (2.8%)	11.173* (2.6%)	0.506 (3.2%)	4.202 (5.8%)	6.630* (3.2%)	1.217 (1.0%)	10.753 (3.3%)	15.058* (6.9%)
	ours (s)	0.399 (5.4%)	3.185 (9.8%)	10.460* (9.5%)	0.473 (10.4%)	3.953 (12.4%)	6.198* (10.4%)	1.171 (4.9%)	10.417 (6.7%)	14.376* (11.9%)

Table 3: *Spatial and temporal performance of the new kd-trees. Several scenes with low to high geometric complexity were used to compare the new kd-tree representation with the standard method (*std.*), which is based on the construction and representation methods given in [WH06] and [Wal04], respectively. Two combinations of occupancy and frequency thresholds were tested to produce a fast ray-tracing speed (*ours (f)*) and a small kd-tree size (*ours (s)*).*